

## Research Article

# Passive Localization of 3D Near-Field Cyclostationary Sources Using Parallel Factor Analysis

Jian Chen, Guohong Liu, and Xiaoying Sun

*College of Communication and Engineering, Jilin University, Changchun 130022, China*

Correspondence should be addressed to Jian Chen; [chenjian@jlu.edu.cn](mailto:chenjian@jlu.edu.cn)

Received 6 February 2013; Accepted 2 June 2013

Academic Editor: Krzysztof Kulpa

Copyright © 2013 Jian Chen et al. This is an open access article distributed under the Creative Commons Attribution License, which permits unrestricted use, distribution, and reproduction in any medium, provided the original work is properly cited.

By exploiting favorable characteristics of a uniform cross-array, a passive localization algorithm of narrowband cyclostationary sources in the spherical coordinates (azimuth, elevation, and range) is proposed. Firstly, we construct a parallel factor (PARAFAC) analysis model by computing the third-order cyclic moment matrices of the properly chosen sensor outputs. Then, we analyze the uniqueness of the constructed model and obtain three-dimensional (3D) near-field parameters via trilinear alternating least squares regression (TALS). The investigated algorithm is well suitable for the localization of the near-field cyclostationary sources. In addition, it avoids the multidimensional search and pairing parameters. Results of computer simulations are carried out to confirm the satisfactory performance of the proposed method.

## 1. Introduction

There has been considerable interest in bearing estimation for radar, sonar, communication, and electronic surveillance [1]. Various high-resolution algorithms, such as MUSIC [2] and ESPRIT [3], have been proposed to obtain the direction-of-arrival estimation of the far-field sources. In addition, when the sources are localized at the Fresnel region [4] of the array aperture, both the azimuth and range should be estimated. Recently, a significant amount attention has been paid to this issue and several near-field sources localization algorithms [5–7] are also available. However, all these methods as mentioned above only address the 2D problem of estimating azimuth and range and rely on the assumption of the stationary sources.

In recent years, several 3D near-field sources localization methods have been developed to obtain azimuth, elevation, and range. Meraim and Hua [8] proposed a second-order based method to cope with this issue. By translating the 1D uniform linear array of near field into a virtual rectangular array of virtual far field, Challa and Shamsunder [9] developed a fourth-order cumulants based Unitary-ESPRIT method. Moreover, [10, 11] also introduced efficient localization methods for 3-D near-field non-Gaussian stationary

sources. It is obviously seen that all these methods still require that the incoming signals should be stationary ones; in addition, a multidimensional search or pairing parameters is also failed to avoid.

Cyclostationarity, which is a statistical property processed by most man-made communication signals, is related to the underlying periodicity arising from cyclic frequency of based rates. Besson et al. [12] introduced an original far-field approximation [13] based method to deal with the bearings estimation of near-field cyclostationary sources. Due to the fact that the effect caused by the mismatch between the actual spherical wavefront phase vector and assumed planar wavefront vector was alleviated, the proposed technique showed a satisfactory performance for the near-field sources far away from the sensor array. The estimations for elevation and range, however, have not been well considered.

In this paper, we consider the problem of jointly estimating elevation, azimuth, and range of the near-field cyclostationary sources; what is more, a two-stage passive localization method has been proposed. In the first stage, several third-order cyclic moment matrices of a cross-array observations data are computed, and a parallel factor analysis model in the cyclic statistic domain is constructed. In the second stage, the uniqueness of the constructed model is proved;

in addition, the 3-D localizing parameters for the near-field sources have also been obtained through TALS. The algorithm developed in this paper would be well suitable for near-field cyclostationary sources, and it does not require multidimensional search or pairing parameters; in addition, it also can effectively alleviate the array aperture loss.

The rest of this paper is organized as follows. Section 2 introduces the signal model of near-field localization based on cross-array. Section 3 develops a joint estimation algorithm of three parameters in near-field. Section 4 shows simulation results. Section 5 presents the conclusion of the whole paper.

## 2. Near-Field Signal Model Based Cross-Array

*2.1. Near-Field Signal Model.* We consider a near-field scenario of  $M$  uncorrelated narrowband signals impinging on a cross-array signed with the  $x$  and  $y$  axes (Figure 1), which consists of  $L = 2N + 3$  sensors with element spacing  $d$ .

Let the array center be the phase reference point, and the signals received by the  $(l, 0)$ th and the  $(0, l)$ th can be, respectively, expressed as

$$\begin{aligned} x_{l,0}(t) &= \sum_{m=1}^M s_m(t) \exp(j(\gamma_{xm}l + \varphi_{xm}l^2)) + n_{l,0}(t), \\ x_{0,l}(t) &= \sum_{m=1}^M s_m(t) \exp(j(\gamma_{ym}l + \varphi_{ym}l^2)) + n_{0,l}(t), \end{aligned} \quad (1)$$

where  $n(t)$  donates the sensor additive noise, and

$$\begin{aligned} \gamma_{xm} &= -2\pi \frac{d}{\lambda} \sin \alpha_m \cos \theta_m, \\ \varphi_{xm} &= \pi \frac{d^2}{\lambda r_m} (1 - \sin^2 \alpha_m \cos^2 \theta_m), \\ \gamma_{ym} &= -2\pi \frac{d}{\lambda} \sin \alpha_m \sin \theta_m, \\ \varphi_{ym} &= \pi \frac{d^2}{\lambda r_m} (1 - \sin^2 \alpha_m \sin^2 \theta_m), \end{aligned} \quad (2)$$

where  $\alpha_m$ ,  $\theta_m$ , and  $r_m$  indicate elevation, azimuth, and range of  $m$ th signal, respectively, and  $\lambda$  is wavelength of source signal.

The  $m$ th source signal with amplitude  $z_m(t)$  can be modeled as

$$s_m(t) = z_m(t) \exp(j\omega t) \quad m = 1, 2, \dots, M, \quad (3)$$

where  $\bar{\omega}$  is the center frequency.

*2.2. Assumption of Signal Model.* The main problem addressed in this paper is to jointly estimate the sets of parameters  $(\alpha_m, \theta_m, \text{ and } r_m)$ , and then the following assumptions are assumed to hold:

- (1) the envelope  $z_m(t)$  is non-Gaussian stationary random process with zero mean and nonzero skewness;
- (2) the sensor noise is the additive stationary one and independent from the source signals;

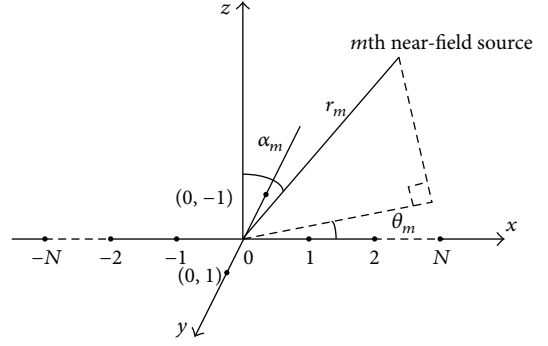


FIGURE 1: Sensor-source configuration for the near-field problem.

- (3) the sensor array is a uniform linear array with element spacing  $d \leq \lambda/4$ ; in addition, the source number  $M$  is not more than sensor number  $N$ .

*2.3. Parallel Factor Analysis.* We need to introduce the following notation that will be used in the sequel.

*Definition 1* (see [14]). Let  $x_{k,n,p}$  stand for the  $(k, n, p)$  element of a three-dimensional tensor  $\mathbf{X}$ , if

$$x_{k,n,p} = \sum_{m=1}^M a_{k,m} b_{n,m} c_{p,m}, \quad (4)$$

where  $a_{k,m}$  denotes the  $(k, m)$  element of matrix  $\mathbf{A}$  and similarly for the others. Equation (4) indicates  $x_{k,n,p}$  as a sum of triple products, which is variably known as the trilinear model, trilinear decomposition, triple product decomposition, canonical decomposition, or parallel factor (PARAFAC) analysis.

*Definition 2* (see [14]). For a matrix  $\mathbf{B} \in C^{I \times J}$ , if all  $I < J$  columns of  $\mathbf{B}$  are linearly independent, but there exists a collection of  $I + 1$  linearly dependent columns of  $\mathbf{B}$ , then it has Kruskal-rank ( $k$ -rank)  $k_{\mathbf{B}} = I$ .

*Theorem 3* (see [15]). Consider a three dimensional tensor  $\mathbf{X}$  as defined in (4), and  $M$  represents the common dimension, if

$$k_{\mathbf{A}} + k_{\mathbf{B}} + k_{\mathbf{C}^T} \geq 2M + 2, \quad (5)$$

then  $\mathbf{A}$ ,  $\mathbf{B}$ , and  $\mathbf{C}$  are unique up to permutation and (complex) scaling of columns.

## 3. PARAFAC Based 3D Near-Field Sources Localization

*3.1. Compute the Third-Order Cyclic Moments Matrices.* Let  $M_{3,x}^a(0, -l-1, -l)$  denote the third-order cyclic moment with cyclic frequency  $\alpha$  defined as

$$\begin{aligned} M_{3,x}^a(0, -l-1, -l) &= \lim_{T \rightarrow \infty} \frac{1}{T} \sum_{t=1}^T E \{ x_{0,0}(t) x_{-l-1,0}(t) x_{-l,0}^*(t) \} \exp(-j\alpha t), \end{aligned} \quad (6)$$

where the superscript “\*” denotes the complex conjugate operation; in addition,  $E\{x_{0,0}(t)x_{-l-1,0}(t)x_{-l,0}^*(t)\}$  can be given by

$$\begin{aligned}
& E\{x_{0,0}(t)x_{-l-1,0}(t)x_{-l,0}^*(t)\} \\
&= \sum_{m=1}^M m_{3,z_m} \exp(j(-\gamma_{xm} + \phi_{xm})) \exp(j2\phi_{xm}l) \exp(j\omega t) \\
&\quad + m_{1,n} \sum_{m=1}^M m_{2,z_m} \exp(j[\gamma_{xm}(-l-1) + \phi_{xm}(-l-1)^2]) \\
&\quad \quad \times \exp(j2\omega t) \\
&\quad + m_{1,n} \sum_{m=1}^M m_{2,z_m} \exp(-j[\gamma_{xm}(-l) + \phi_{xm}(-l)^2]) \\
&\quad + m_{2,n} \sum_{m=1}^M m_{1,z_m} \exp(j\omega t) \\
&\quad + m_{1,n} \sum_{m=1}^M m_{2,z_m} \exp(j(-\gamma_{xm} + \phi_{xm})) \exp(j2\phi_{xm}l) \\
&\quad + m_{2,n} \sum_{m=1}^M m_{1,z_m} \exp(j[\gamma_{xm}(-l-1) + \phi_{xm}(-l-1)^2]) \\
&\quad \quad \times \exp(j\omega t) \\
&\quad + m_{2,n} \sum_{m=1}^M m_{1,z_m} \exp(-j[\gamma_{xm}(-l) + \phi_{xm}(-l)^2]) \\
&\quad \quad \times \exp(j\omega t) + m_{3,n}, \tag{7}
\end{aligned}$$

where  $m_{1,z_m}$ ,  $m_{2,z_m}$ , and  $m_{3,z_m}$  denote mean, variance, and the third-order moment of  $z_m(t)$ ; in addition,  $m_{1,n}$ ,  $m_{2,n}$ , and  $m_{3,n}$  represent mean, variance, and the third-order cyclic moment of  $n(t)$ , respectively.

With assumption being considered, we further obtain

$$\begin{aligned}
& M_{3,x}^a(0, -l-1, -l) \\
&= \sum_{m=1}^M m_{3,z_m} \exp(j(-\gamma_{xm} + \phi_{xm})) \exp(j2\phi_{xm}l) \delta(\omega - \alpha) \\
&\quad + m_{1,n} \sum_{m=1}^M m_{2,z_m} \exp(j[\gamma_{xm}(-l-1) + \phi_{xm}(-l-1)^2]) \\
&\quad \quad \times \delta(2\omega - \alpha) \\
&\quad + m_{1,n} \sum_{m=1}^M m_{2,z_m} \exp(-j[\gamma_{xm}(-l) + \phi_{xm}(-l)^2]) \delta(\alpha) \\
&\quad + m_{1,n} \sum_{m=1}^M m_{2,z_m} \exp(j(-\gamma_{xm} + \phi_{xm})) \exp(j2\phi_{xm}l) \delta(\alpha) \\
&\quad \quad + m_{3,n} \delta(\alpha), \tag{8}
\end{aligned}$$

where  $\delta$  is impulse function. Letting  $a = \bar{\omega}$  and substituting (8) into (6) yield

$$\begin{aligned}
& M_{3,x}^a(0, -l-1, -l) \\
&= \sum_{m=1}^M m_{3,z_m} \exp(j(-\gamma_{xm} + \phi_{xm})) \exp(j2l\phi_{xm}). \tag{9}
\end{aligned}$$

Based on (9), we reconstruct the spatial third-order cyclic moment matrix  $\mathbf{M}_1^a$ , in which the  $(k, q)$ th element can be expressed as follows:

$$\begin{aligned}
\mathbf{M}_1^a(k, q) &= M_{3,x}^a(0, q-k-1, q-k) \\
&= \sum_{m=1}^M m_{3,z_m} \exp(j(-\gamma_{xm} + \phi_{xm})) \\
&\quad \quad \times \exp(j2(k-q)\phi_{xm}). \tag{10}
\end{aligned}$$

In a matrix form, (10) can be written as

$$\mathbf{M}_1^a = \mathbf{A} \mathbf{M}_z^a \mathbf{\Omega}_1^* \mathbf{\Phi}_1 \mathbf{A}^H, \tag{11}$$

where the superscript “ $H$ ” represents conjugate transpose operation,  $\mathbf{M}_z^a$  denotes the third-order moment matrix of source signals, and

$$\begin{aligned}
\mathbf{A} &= [\mathbf{a}_1, \mathbf{a}_2, \dots, \mathbf{a}_M], \\
\mathbf{a}_m &= [1, \exp(j2\phi_{xm}), \dots, \exp(j2(N-1)\phi_{xm})], \\
\mathbf{\Omega}_1 &= \text{diag}(\exp(j\gamma_{x1}), \exp(j\gamma_{x2}), \dots, \exp(j\gamma_{xM})), \\
\mathbf{\Phi}_1 &= \text{diag}(\exp(j\phi_{x1}), \exp(j\phi_{x2}), \dots, \exp(j\phi_{xM})). \tag{12}
\end{aligned}$$

On the other hand, following the same process described above, we can easily obtain

$$\begin{aligned}
& M_{3,x}^a(0, l+1, l) \\
&= m_{3,u} \sum_{m=1}^M m_{3,z_m} \exp(j(\gamma_{xm} + \phi_{xm})) \exp(j2l\phi_{xm}), \\
& M_{3,x}^a(1, -l-1, -l) \\
&= m_{3,u} \sum_{m=1}^M m_{3,z_m} \exp(j(-\gamma_{xm} + \phi_{xm})) \\
&\quad \quad \times \exp(j(\gamma_{ym} + \phi_{ym})) \exp(j2l\phi_{xm}), \\
& M_{3,x}^a(-1, -l-1, -l) \\
&= m_{3,u} \sum_{m=1}^M m_{3,z_m} \exp(j(-\gamma_{xm} + \phi_{xm})) \\
&\quad \quad \times \exp(j(-\gamma_{ym} + \phi_{ym})) \exp(j2l\phi_{xm}). \tag{13}
\end{aligned}$$

And the elements of the other three matrices can be expressed as

$$\begin{aligned}
\mathbf{M}_2^a(k, q) &= M_{3,x}^a(0, k - q + 1, k - q) \\
&= \sum_{m=1}^M m_{3,z_m} \exp(j(\gamma_{xm} + \varphi_{xm})) \exp(j2(k - q)\varphi_{xm}), \\
\mathbf{M}_3^a(k, q) &= M_{3,x}^a(1, q - k - 1, q - k) \\
&= \sum_{m=1}^M m_{3,z_m} \exp(j(-\gamma_{xm} + \varphi_{xm})) \\
&\quad \times \exp(j(\gamma_{ym} + \varphi_{ym})) \exp(j2(k - q)\varphi_{xm}), \\
\mathbf{M}_4^a(k, q) &= M_{3,x}^a(-1, q - k - 1, q - k) \\
&= \sum_{m=1}^M m_{3,z_m} \exp(j(-\gamma_{xm} + \varphi_{xm})) \\
&\quad \times \exp(j(-\gamma_{ym} + \varphi_{ym})) \exp(j2(k - q)\varphi_{xm}).
\end{aligned} \tag{14}$$

Finally, we have

$$\begin{aligned}
\mathbf{M}_2^a &= \mathbf{A} \mathbf{M}_z^a \Omega_1 \Phi_1 \mathbf{A}^H, \\
\mathbf{M}_3^a &= \mathbf{A} \mathbf{M}_z^a \Omega_1^* \Phi_1 \Omega_2 \Phi_2 \mathbf{A}^H, \\
\mathbf{M}_4^a &= \mathbf{A} \mathbf{M}_z^a \Omega_1^* \Phi_1 \Omega_2 \Phi_2 \mathbf{A}^H
\end{aligned} \tag{15}$$

with

$$\begin{aligned}
\Omega_2 &= \text{diag}(\exp(j\gamma_{y1}), \exp(j\gamma_{y2}), \dots, \exp(j\gamma_{yM})), \\
\Phi_2 &= \text{diag}(\exp(j\varphi_{y1}), \exp(j\varphi_{y2}), \dots, \exp(j\varphi_{yM})).
\end{aligned} \tag{16}$$

**3.2. Build the Parallel Factor Analysis Model.** Considering the situation of limited samples, we build a parallel factor analysis model that uses the third-order cyclic moments as

$$\begin{aligned}
\widetilde{\mathbf{M}}^a &= \begin{bmatrix} \widetilde{\mathbf{M}}^a(:, :, 1) \\ \widetilde{\mathbf{M}}^a(:, :, 2) \\ \widetilde{\mathbf{M}}^a(:, :, 3) \\ \widetilde{\mathbf{M}}^a(:, :, 4) \end{bmatrix} = \begin{bmatrix} \widetilde{\mathbf{M}}_1^a \\ \widetilde{\mathbf{M}}_2^a \\ \widetilde{\mathbf{M}}_3^a \\ \widetilde{\mathbf{M}}_4^a \end{bmatrix} = \begin{bmatrix} \mathbf{A} \mathbf{M}_z^a \Omega_1^* \Phi_1 \mathbf{A}^H \\ \mathbf{A} \mathbf{M}_z^a \Omega_1 \Phi_1 \mathbf{A}^H \\ \mathbf{A} \mathbf{M}_z^a \Omega_1^* \Phi_1 \Omega_2 \Phi_2 \mathbf{A}^H \\ \mathbf{A} \mathbf{M}_z^a \Omega_1^* \Phi_1 \Omega_2^* \Phi_2 \mathbf{A}^H \end{bmatrix} + \nu_1
\end{aligned} \tag{17}$$

with  $\mathbf{C} = \mathbf{A}^*$ , and the Khatri-Rao product [15] for (17) shows

$$\widetilde{\mathbf{M}}^a = (\mathbf{D} \otimes \mathbf{A}) \mathbf{C}^T + \nu_1, \tag{18}$$

where

$$\mathbf{D} = \begin{bmatrix} g^{-1}(\mathbf{M}_z^a \Omega_1^* \Phi_1) \\ g^{-1}(\mathbf{M}_z^a \Omega_1 \Phi_1) \\ g^{-1}(\mathbf{M}_z^a \Omega_1^* \Phi_1 \Omega_2 \Phi_2) \\ g^{-1}(\mathbf{M}_z^a \Omega_1^* \Phi_1 \Omega_2^* \Phi_2) \end{bmatrix}, \tag{19}$$

with  $g^{-1}(\mathbf{M}_z^a \Omega_1^* \Phi_1)$  denoting a row vector consisting of diagonal matrix  $\mathbf{M}_z^a \Omega_1^* \Phi_1$ .

Similarly, (18) also yields

$$\begin{aligned}
\widetilde{\mathbf{X}} &= (\mathbf{A} \otimes \mathbf{C}) \mathbf{D}^T + \nu_2, \\
\widetilde{\mathbf{Y}} &= (\mathbf{C} \otimes \mathbf{D}) \mathbf{A}^T + \nu_3.
\end{aligned} \tag{20}$$

**3.3. Solve the Parallel Factor Analysis Model, and Estimate 3-D Parameters.** As it stands,  $\mathbf{A}$  and  $\mathbf{C}$  are both Vandermonde matrices, and then they have Kruskal-rank ( $k$ -rank)  $k_{\mathbf{A}} = k_{\mathbf{C}^T} = M$ . On the other hand, the  $k$ -rank of  $\mathbf{D}$  will be  $k_{\mathbf{D}} = \min(4, M)$ . When the condition that the number of signals being  $M \geq 2$  holds, then  $\mathbf{A}$ ,  $\mathbf{C}$ , and  $\mathbf{D}$  are unique up to permutation and scaling of columns. With trilinear alternating least squares regression, we obtain that

$$\begin{aligned}
\widetilde{\mathbf{C}}^T &= \arg \min_{\mathbf{C}^T} \|\widetilde{\mathbf{M}}^a - (\mathbf{D} \otimes \mathbf{A}) \mathbf{C}^T\|_F^2, \\
\widetilde{\mathbf{D}}^T &= \arg \min_{\mathbf{D}^T} \|\widetilde{\mathbf{X}} - (\mathbf{A} \otimes \mathbf{C}) \mathbf{D}^T\|_F^2, \\
\widetilde{\mathbf{A}}^T &= \arg \min_{\mathbf{A}^T} \|\widetilde{\mathbf{Y}} - (\mathbf{C} \otimes \mathbf{D}) \mathbf{A}^T\|_F^2.
\end{aligned} \tag{21}$$

Then using these estimates, we can associate with each pair  $(\gamma_{xm}, \gamma_{ym}, \text{ and } \varphi_{ym})$  as follows:

$$\begin{aligned}
\widetilde{\gamma}_{xm} &= \frac{1}{2} \arg \left( \frac{\widetilde{\mathbf{D}}(2, m)}{\widetilde{\mathbf{D}}(1, m)} \right), \\
\widetilde{\gamma}_{ym} &= \frac{1}{2} \left\{ \arg \left( \frac{\widetilde{\mathbf{D}}(3, m)}{\widetilde{\mathbf{D}}(1, m)} \right) - \arg \left( \frac{\widetilde{\mathbf{D}}(4, m)}{\widetilde{\mathbf{D}}(1, m)} \right) \right\}, \\
\widetilde{\varphi}_{ym} &= \frac{1}{2} \left\{ \arg \left( \frac{\widetilde{\mathbf{D}}(3, m)}{\widetilde{\mathbf{D}}(1, m)} \right) + \arg \left( \frac{\widetilde{\mathbf{D}}(4, m)}{\widetilde{\mathbf{D}}(1, m)} \right) \right\}.
\end{aligned} \tag{22}$$

Finally, the sources parameters can be estimated as

$$\widetilde{\alpha}_m = \text{asin} \left( \frac{\lambda}{2\pi d} (\widetilde{\gamma}_{xm}^2 + \widetilde{\gamma}_{ym}^2)^{1/2} \right), \tag{23}$$

$$\widetilde{\theta}_m = \text{atan} \left( \frac{\widetilde{\gamma}_{ym}}{\widetilde{\gamma}_{xm}} \right), \tag{24}$$

$$\widetilde{r}_m = \frac{\pi d^2 (1 - \sin^2 \widetilde{\alpha}_m \sin^2 \widetilde{\theta}_m)}{\lambda \widetilde{\varphi}_{ym}}. \tag{25}$$

## 4. Computer Simulation Results

In this section, we explicit some simulation results to evaluate the performance of proposed method. For all examples, a uniform linear array with number of 15 sensors and element spacing  $0.25\lambda$  is displayed, where  $\lambda$  is the wavelength of the narrowband source signals. Two near-field or far-field equal power cyclostationary signals are impinging on the array with center frequency  $0.25\pi$ , and their envelopes can be modeled as exponentially distributed. To be compared, we simultaneously execute the method of [12], which is suitable for the

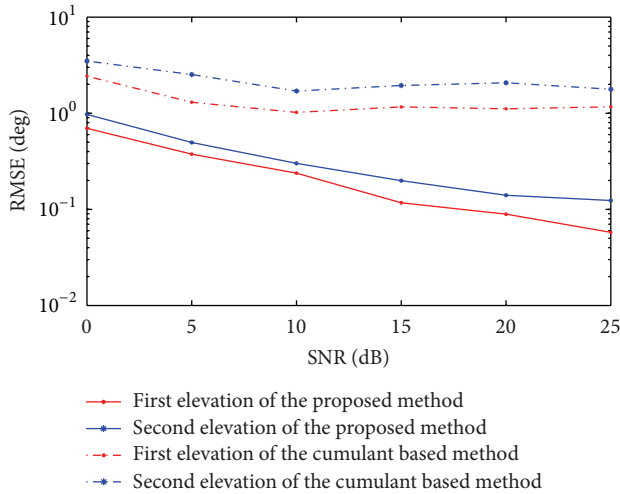


FIGURE 2: The RMSE of elevation estimations for two near-field sources using the proposed method and the cumulant based method versus SNR.

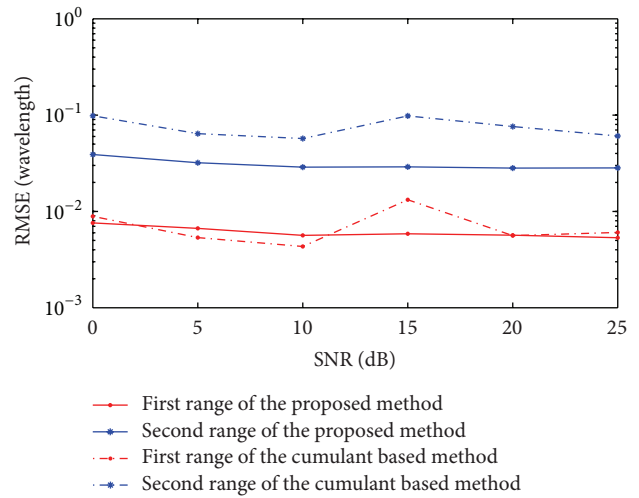


FIGURE 4: The RMSE of range estimations for two near-field sources using the proposed method and the cumulant based method versus SNR.

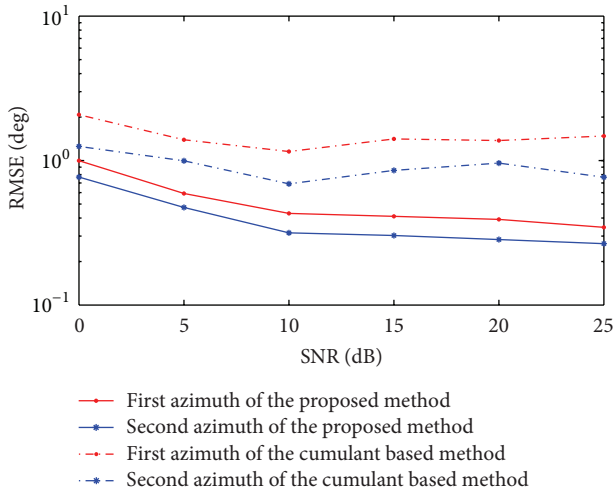


FIGURE 3: RMSE of azimuth estimations for two near-field sources using the proposed method and the cumulant based method versus SNR.

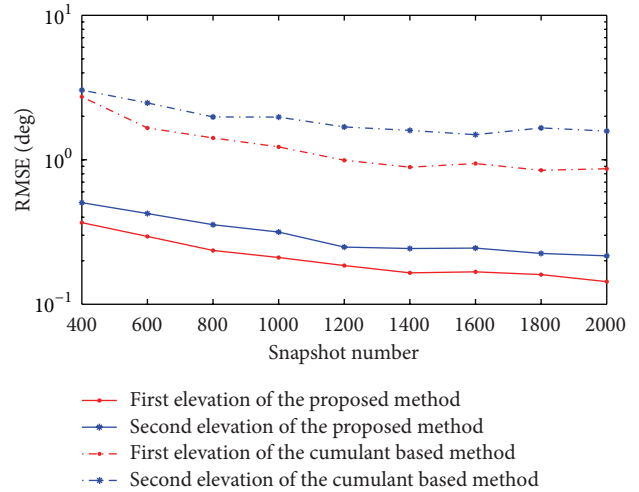


FIGURE 5: The RMSE of elevation estimations for two near-field sources using the proposed method and the cumulant based method versus snapshot number.

3-D near-field non-Gaussian stationary sources localization. The presented results are evaluated by the estimated root mean square error (RMSE) from the averaged results of 200 independent Monte-Carlo simulations.

In the first example, Two near-field sources are located at  $(35^\circ, 46^\circ, \text{ and } 1/6\lambda)$  and  $(20^\circ, 60^\circ, \text{ and } 2/5\lambda)$ , respectively. The additive noise is time and spatially white Gaussian with zero mean and unit variance. In addition, the snapshot number is set equal to 1024. When SNR varies from 0 dB to 25 dB, the RMSE of the elevation, azimuth, and range estimations for two near-field cyclostationary sources can be shown in Figures 2, 3, and 4. For the comparison, the performance in the same situation for the fourth-order cumulants based method has also been displayed. From these three figures, it is obvious that the proposed method performs better in elevation, azimuth, and range estimation than the FFA based

algorithm for all SNRs. What is more, the RMSE of range estimations for the first source that is closer to the array is less than the second one. This phenomenon is well agreement with the theoretical analysis that the sources closer to sensor array would hold a smaller standard deviation than the one far from the array [7].

In the second example, the simulation condition is similar to the first example, except that the SNR is set at 10 dB, and the snapshot number is varied from 400 to 2000. The RMSE of elevation, azimuth, and range estimations of two near-field cyclostationary sources obtained from the proposed method as well as the cumulant based method can be displayed in Figures 5, 6, and 7. From these three figures, we can see that the proposed method still shows a more satisfactory accuracy than the cumulant based method in all available snapshots. In addition, the range estimations for the first sources are

TABLE 1: RMSE of 3D parameters for near-field localization in the third example.

Example	Source	True	Mean	Variance	Source	True	Mean	Variance
White noise	$\alpha_1$	$35^\circ$	$34.95^\circ$	0.1923	$\alpha_2$	$20^\circ$	$20.03^\circ$	0.1647
	$\theta_1$	$40^\circ$	$39.99^\circ$	0.0419	$\theta_2$	$60^\circ$	$59.99^\circ$	0.1000
	$r_1$	$\lambda/6$	$0.1669\lambda$	$3.5744 \times 10^{-5}$	$r_2$	$2\lambda/5$	$0.3984\lambda$	$8.2107 \times 10^{-4}$
Colored noise	$\alpha_1$	$35^\circ$	$35.02^\circ$	0.2146	$\alpha_2$	$20^\circ$	$19.98^\circ$	0.0618
	$\theta_1$	$40^\circ$	$40.03^\circ$	0.0795	$\theta_2$	$60^\circ$	$60.02^\circ$	0.1165
	$r_1$	$\lambda/6$	$0.1662\lambda$	$2.8455 \times 10^{-5}$	$r_2$	$2\lambda/5$	$0.4036\lambda$	$8.4173 \times 10^{-4}$

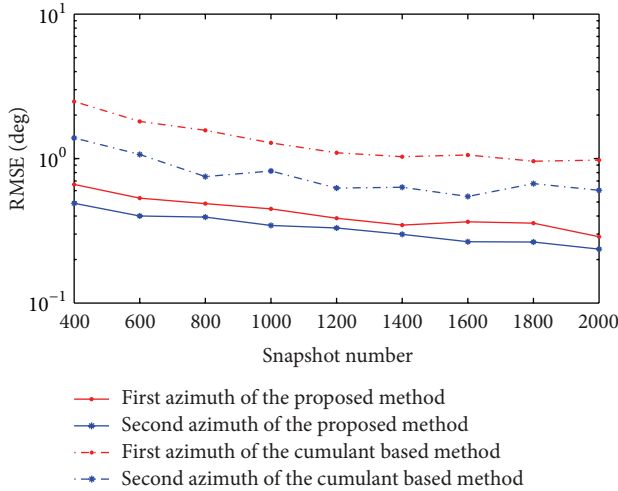


FIGURE 6: The RMSE of azimuth estimations for two near-field sources using the proposed method and the cumulant based method versus snapshot number.

much better than the second one, while the elevation and azimuth estimations for both near-field sources are similar for the proposed method.

In the third example, the additive noise is time and spatially white Gaussian random process and the colored noise from a second-order AR model with parameter  $(-1.8, 0.9)$ , respectively. In addition, the other simulation condition is similar to the first example, except that the SNR is set at 10 dB, and snapshot number is equal to 1024. The mean and variance of the elevation, azimuth, and range estimations for two near-field cyclostationary sources can be shown in Table 1. From this table, we can easily see that the effectiveness of the proposed method is not little affected by the difference of the sensor noise.

## 5. Conclusion

This paper considers the problem of the passive localization of 3-D near-field cyclostationary sources and proposes an efficient third-order cyclic moment based algorithm. The construction of the parallel factor analysis model in the cyclic domain avoids the multidimensional search and pairing parameters. Moreover, the utilization of trilinear alternating least squares regression deals with the joint estimation of elevation, azimuth, and range. From the simulation results

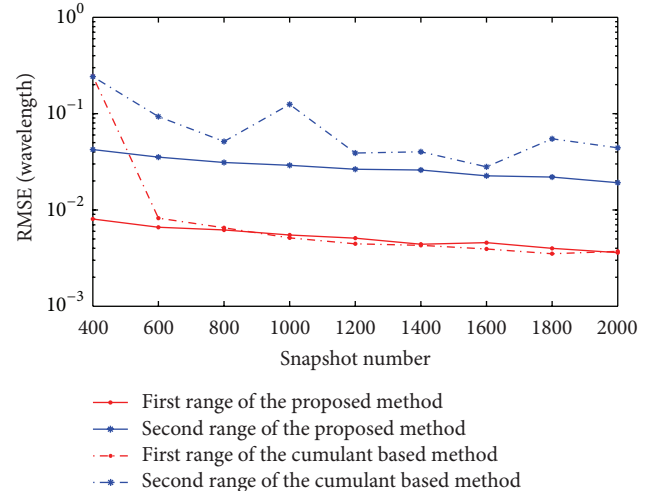


FIGURE 7: The RMSE of range estimations for two near-field sources using the proposed method and the cumulant based method versus snapshot number.

mentioned above, the proposed method outperforms the cumulant based method in locating near-field cyclostationary sources; in addition, the stationary noise has a little influence on the estimated accuracy of the proposed method.

## Acknowledgments

This work is supported by the National Natural Science Foundation of China (61171137) and Specialized Research Fund for the Doctoral Program of Higher Education (20090061120042).

## References

- [1] J. Liang, X. Zeng, B. Ji, J. Zhang, and F. Zhao, "A computationally efficient algorithm for joint range-DOA-frequency estimation of near-field sources," *Digital Signal Processing*, vol. 19, no. 4, pp. 596–611, 2009.
- [2] H. Krim and M. Viberg, "Two decades of array signal processing research: the parametric approach," *IEEE Signal Processing Magazine*, vol. 13, no. 4, pp. 67–94, 1996.
- [3] A. J. Weiss and B. Friedlander, "Range and bearing estimation using polynomial rooting," *IEEE Journal of Oceanic Engineering*, vol. 18, no. 2, pp. 130–137, 1993.
- [4] W. Zhi and M. Y.-W. Chia, "Near-field source localization via symmetric subarrays," in *Proceedings of the IEEE International*

- Conference on Acoustics, Speech and Signal Processing (ICASSP '07)*, pp. III121–III124, Honolulu, Hawaii, USA, April 2007.
- [5] D. Starer and A. Nehorai, “Path-following algorithm for passive localization of near-field sources,” in *Proceedings of the 5th ASSP Workshop on Spectrum Estimation and Modeling*, pp. 322–326, 1990.
- [6] D. Starer and A. Nehorai, “Passive localization on near-field sources by path following,” *IEEE Transactions on Signal Processing*, vol. 42, no. 3, pp. 677–680, 1994.
- [7] R. A. Harshman, “Foundation of the PARAFAC procedure: model and conditions for an explanatory mutil-mode factor analysis,” *UCLA Working Papers in Phonetics*, vol. 22, no. 7, pp. 111–117, 1972.
- [8] K. Aberd Meraim and Y. Hua, “3-D near field source localization using second order statistics,” in *Proceedings of 31st Alisomar Conference on Signals, Systems and Computers*, vol. 2, pp. 1307–1310, 1997.
- [9] R. N. Challa and S. Shamsunder, “Passive near-field localization of multiple non-Gaussian sources in 3-D using cumulants,” *Signal Processing*, vol. 65, no. 1, pp. 39–53, 1998.
- [10] K. Deng and Q. Yin, “Closed form parameters estimation for 3-D near field sources,” in *Proceedings of the IEEE International Conference on Acoustics, Speech and Signal Processing (ICASSP '06)*, pp. IV1133–IV1136, Toulouse, France, May 2006.
- [11] C. M. Lee, K. S. Yoo, and K. K. Lee, “Efficient algorithm for localizing 3-D narrowband multiple sources,” *IEE Proceedings of Radar, Sonar and Navigation*, vol. 38, no. 1, pp. 23–26, 2001.
- [12] O. Besson, P. Stoica, and A. B. Gershman, “Simple and accurate direction of arrival estimator in the case of imperfect spatial coherence,” *IEEE Transactions on Signal Processing*, vol. 49, no. 4, pp. 730–737, 2001.
- [13] A. L. Swindlehurst and T. Kailath, “A performance analysis of subspace-based methods in the presence of model errors—I: the MUSIC algorithm,” *IEEE Transactions on Signal Processing*, vol. 40, no. 7, pp. 1758–1774, 1992.
- [14] N. D. Sidiropoulos, R. Bro, and G. B. Giannakis, “Parallel factor analysis in sensor array processing,” *IEEE Transactions on Signal Processing*, vol. 48, no. 8, pp. 2377–2388, 2000.
- [15] J.-L. Liang, B.-J. Ji, F. Zhao, and J.-Y. Zhang, “Near-field source localization algorithm using parallel factor analysis,” *Acta Electronica Sinica*, vol. 35, no. 10, pp. 1909–1915, 2007.

